Quantification of circulating *Mycobacterium tuberculosis* antigen peptides allows rapid diagnosis of active disease and treatment monitoring

Chang Liu[a,b,c], Zhen Zhao[d], Jia Fan[a,c], Christopher J. Lyon[a,c], Hung-Jen Wu[a,e], Dobrin Nedelkov[f], Adrian M. Zelazny[d], Kenneth N. Olivier[g], Lisa H. Cazares[h], Steven M. Holland[i], Edward A. Graviss[j], and Ye Hu[a,b,c,1]

[a]Department of Nanomedicine, Houston Methodist Research Institute, Houston, TX 77030; [b]School of Biological and Health Systems Engineering, Arizona State University, Tempe, AZ 85287; [c]Virginia G. Piper Biodesign Center for Personalized Diagnostics, The Biodesign Institute, Arizona State University, Tempe, AZ 85287; [d]Department of Laboratory Medicine, Clinical Center, National Institutes of Health, Bethesda, MD 20892; [e]Department of Chemical Engineering, Texas A&M University, College Station, TX 77843; [f]Molecular Biomarkers Laboratory, The Biodesign Institute, Arizona State University, Tempe, AZ 85287; [g]Cardiovascular and Pulmonary Branch, National Heart, Lung, and Blood Institute, Bethesda, MD 20892; [h]Molecular and Translational Sciences, US Army Medical Research Institute of Infectious Diseases, Frederick, MD 21702; [i]Laboratory of Clinical Infectious Diseases, National Institute of Allergy and Infectious Diseases, Bethesda, MD 20892; and [j]Department of Pathology and Genomic Medicine, Houston Methodist Research Institute, Houston, TX 77030

Edited by William R. Jacobs Jr., Albert Einstein College of Medicine, Howard Hughes Medical Institute, Bronx, NY, and approved February 17, 2017 (received for review January 6, 2017)

Tuberculosis (TB) is a major global health threat, resulting in an urgent unmet need for a rapid, non–sputum-based quantitative test to detect active *Mycobacterium tuberculosis* (*Mtb*) infections in clinically diverse populations and quickly assess *Mtb* treatment responses for emerging drug-resistant strains. We have identified *Mtb*-specific peptide fragments and developed a method to rapidly quantify their serum concentrations, using antibody-labeled and energy-focusing porous discoidal silicon nanoparticles (nanodisks) and high-throughput mass spectrometry (MS) to enhance sensitivity and specificity. NanoDisk-MS diagnosed active *Mtb* cases with high sensitivity and specificity in a case-control study with cohorts reflecting the complexity of clinical practice. Similar robust sensitivities were obtained for cases of culture-positive pulmonary TB (PTB; 91.3%) and extrapulmonary TB (EPTB; 92.3%), and the sensitivities obtained for culture-negative PTB (82.4%) and EPTB (75.0%) in HIV-positive patients significantly outperformed those reported for other available assays. NanoDisk-MS also exhibited high specificity (87.1–100%) in both healthy and high-risk groups. Absolute quantification of serum *Mtb* antigen concentration was informative in assessing responses to antimycobacterial treatment. Thus, a NanoDisk-MS assay approach could significantly improve the diagnosis and management of active TB cases, and perhaps other infectious diseases as well.

tuberculosis | blood test | nanodisk | rapid diagnosis | treatment monitoring

Despite international efforts and initiatives, tuberculosis (TB) remains a major public health concern worldwide, associated with high morbidity and mortality (1, 2). Detecting active TB cases and monitoring their responses to therapy are fraught with challenges, relying predominantly on microbiologic techniques that use sputum samples, including acid-fast Bacillus (AFB) smear microscopy—widely used as an initial test for TB diagnosis (3, 4)—and *Mycobacterium tuberculosis* (*Mtb*) culture, both of which have only moderate sensitivity and specificity and a long turnaround time (5, 6). Moreover, sputum samples are difficult to obtain after symptom improvement, and often are not diagnostically useful for extrapulmonary TB (EPTB) cases. The PCR-based Xpert MTB/RIF sputum assay was introduced to improve the speed and specificity of TB diagnosis, but this assay has poor sensitivity under low bacterial loads and cannot distinguish live and nonviable *Mtb* contributions (7, 8). A recent World Health Organization (WHO) policy update acknowledged the low quality of evidence supporting the use of Xpert MTB/RIF to diagnose EPTB (9). Diagnostic challenges can be further magnified in patients coinfected with HIV and TB (10). In addition, none of these techniques provides quantitative results that can be used to monitor treatment effects (11, 12).

Consequently, there is an urgent need, highlighted as a high priority in a recent WHO consensus report (13), for the development of rapid, quantitative, non–sputum-based biomarker tests that do not require bacterial isolation to detect active TB (13). Non–sputum-based IFN-γ release assays (IGRAs), which measure ex vivo immune responses to *Mtb* antigens, have received negative policy recommendations for active TB diagnosis owing to their inability to distinguish active TB and latent TB infection (LTBI), as well as their poor diagnostic performance in HIV/TB-coinfected patients and EPTB patients (14). One recent report used the expression of a set of host innate immune response genes in blood to diagnose pulmonary TB (PTB) cases, but that retrospective study did not examine blood samples of EPTB patients, and could not identify culture-negative TB cases (15). Detection of *Mtb* antigens in patient blood samples can provide direct evidence of TB, but no currently available method has demonstrated adequate diagnostic sensitivity and specificity,

Significance

Active *Mycobacterium tuberculosis* (*Mtb*) infections represent a significant global health threat, but can be difficult to diagnose and manage owing to the nonquantitative nature and relatively poor performance of current frontline sputum-based diagnostic assays, which can be further degraded by certain *Mtb* manifestations. This study describes the development of a rapid and quantitative blood-based assay with high sensitivity and specificity for active *Mtb* infections that can be used to monitor responses to antimycobacterial therapy. Our method combines antibody-labeled, energy-focusing nanodisks with high-throughput mass spectrometry to enhance the detection of *Mtb*-specific peptides in digested serum samples, and should allow rapid clinical translation. This approach also should be applicable to other infectious diseases, particularly those for which conventional immunoassays exhibit suboptimal performance.

Author contributions: C.L., Z.Z., and Y.H. designed research; C.L., J.F., H.-J.W., and D.N. performed research; E.A.G. contributed clinical samples; C.L., Z.Z., J.F., C.J.L., A.M.Z., K.N.O., L.H.C., S.M.H., E.A.G., and Y.H. analyzed data; and C.L., Z.Z., C.J.L., A.M.Z., L.H.C., S.M.H., E.A.G., and Y.H. wrote the paper.

The authors declare no conflict of interest.

This article is a PNAS Direct Submission.

Freely available online through the PNAS open access option.

[1]To whom correspondence should be addressed. Email: tyhu@asu.edu.

This article contains supporting information online at www.pnas.org/lookup/suppl/doi:10.1073/pnas.1621360114/-/DCSupplemental.

likely owing to the epitope-masking effects of host proteins (16) and homology with related antigens of several nontuberculous mycobacteria (NTM) (17, 18).

Here we report a blood-based assay for rapid, specific, and high-sensitivity quantification of active TB infections in patients, which uses antibody-conjugated nanodisks to enrich *Mtb*-specific peptides of 10-kDa culture filtrate protein (CFP-10) and 6-kDa early secretory antigenic target (ESAT-6) from trypsin-digested serum samples. These factors demonstrate homology with those expressed by other Mycobacterium species, but have tryptic peptides that exhibit strong *Mtb* selectivity. Thus, *Mtb*-derived CFP-10 and ESAT-6 serum concentrations appear likely to be strong predictors of active TB disease, because they are actively secreted by virulent mycobacterial strains, can be detected early after *Mtb* infection, and have activities that attenuate mycobacterial clearance (19), implying that their presence in serum can be used to diagnose active *Mtb* infections.

We have incorporated several advances to allow the diagnosis of TB from patient blood samples: identification of *Mtb*-selective CFP-10 and ESAT-6 peptides, and development of antibody-conjugated nanodisks that dramatically increase both target peptide enrichment and matrix-assisted laser desorption/ionization (MALDI) of bound peptides to enhance detection by high-throughput MALDI time-of-flight mass spectrometry (MALDI-TOF MS). Furthermore, trypsin digestion is thought to disrupt protein complexes to release *Mtb* antigens that might be undetectable in conventional immunoassays targeting intact *Mtb* proteins. The NanoDisk-MS method (Fig. 1) permits rapid quantification of serum markers specific for active TB, overcoming obstacles associated with current methodologies, and uses accepted clinical instrumentation to enhance its potential for clinical translation.

We evaluated the diagnostic performance of NanoDisk-MS in HIV-negative and HIV-positive patients drawn from the Houston Tuberculosis Initiative (HTI), a large, population-based TB surveillance study. Results from case-control groups in these populations and longitudinal samples from patients undergoing anti-TB therapy provide strong proof-of-principle evidence supporting the clinical utility of this detection platform.

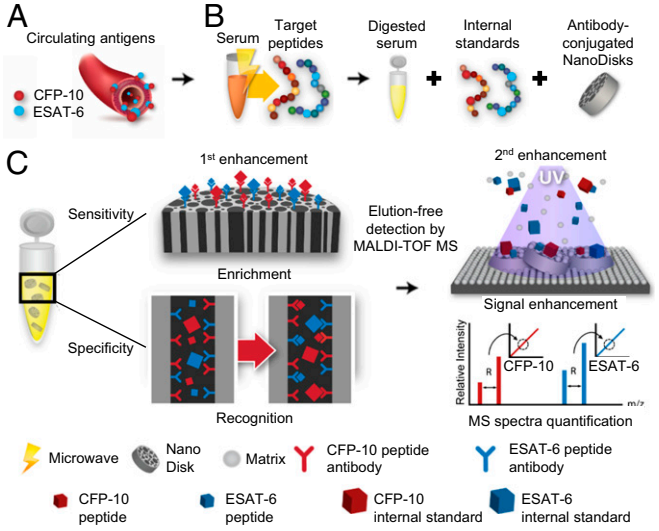

Fig. 1. Schematic illustration of the NanoDisk-MS platform. (*A*) CFP-10 and ESAT-6 are secreted into the circulation from active *Mtb* infections. (*B*) Serum samples are subjected to microwave-assisted tryptic digestion and mixed with functionalized nanodisks and stable isotope-labeled internal standard peptides. (*C*) Peptide quantification. Step 1: Recognition and enrichment of target peptides and stable isotope-labeled internal standard peptides by antibody-conjugated nanodisks. Step 2: A nanodisk effect to enhance MALDI signal allows quantification of target peptide at low concentrations, as determined by MS intensity ratio of target and isotope-labeled internal standard peptides.

Results

Sensitive Nanoparticle-Mediated Detection of *Mtb*-Specific Serum Peptides. Serum CFP-10 and ESAT-6 expression theoretically can be used to diagnose all active *Mtb* infections, including EPTB cases (20); however, some NTM strains express homologs that may reduce the utility of these proteins as biomarkers (21). Since peptide sequence is the gold standard for protein discrimination, we examined whether tryptic peptides could distinguish *Mtb*-derived ESAT-6 and CFP-10 from homologs produced by other species. MALDI-TOF MS analysis of recombinant protein tryptic digests detected CFP-10 (TDAATLAQEAGNFER; *m/z* 1,593.75) and ESAT-6 (WDATATELNNALQNLAR; *m/z* 1,900.95) peptides with high signal-to-noise ratios that were subsequently confirmed by liquid chromatography-tandem mass spectrometry, and which showed strong *Mtb* specificity when aligned with homologs from 12 NTM species (17, 18) (*SI Appendix*, Figs. S1–S3). Both peptides demonstrated perfect homology with *Mycobacterium bovis*, a relatively rare form of TB, but diverged markedly from two species responsible for the majority of NTM infections, *Mycobacterium avium* and *Mycobacterium intracellulare* (22), as well as most other NTM species. The ESAT-6 peptide showed little homology to any NTM, whereas the CFP-10 peptide demonstrated homology only to some strains of *Mycobacterium kansasii*, *Mycobacterium marinum*, and *Mycobacterim ulcerans* that were not expected to significantly interfere with diagnostic specificity in clinical use.

The wide dynamic range of serum protein expression can complicate the cleavage and subsequent detection of low-abundance serum proteins (23). We found that supplemental microwave irradiation allowed serum CFP-10 and ESAT-6 digestion within 20 min instead of overnight, as is normally required for complex protein samples (24), reducing the "sample-to-answer" time to 4 h while increasing the MS signal for target peptides by more than threefold (*SI Appendix*, Fig. S4).

We next analyzed several potential nanoparticle enrichment platforms for their ability to act as MALDI comatrixes that enhance the MS signal by increasing peptide desorption/ionization. MALDI-TOF MS analysis of recombinant CFP-10 and ESAT-6 performed with different nanoparticles showed that gold and silica nanoparticles robustly increased the MS signal, whereas graphene and silver and silicon nanoparticles had negligible to negative effects (Fig. 2*A*). Unlike gold particles, silica particles can be readily modified to precisely control their porosity and thus their surface area and absorbance properties. Thus, we developed a scalable process to rapidly fabricate uniform nanodisks with the surface oxidized to silica to permit antibody functionalization and an absorption spectrum spanning the wavelength of the MALDI-TOF MS UV laser (*SI Appendix*, Fig. S5). Electron microscopy images of these nanodisks revealed highly reproducible 1,000 × 400-nm discs with 40-nm pores coated with a thin silica layer (Fig. 2 *B–D* and *SI Appendix*, Fig. S6). Nanodisks demonstrated the strongest comatrix effect of all tested materials (Fig. 2*A* and *SI Appendix*, Fig. S7), likely owing to their UV absorbance properties and thermal confinement effect to promote laser-induced peptide desorption/ionization and their large surface-to-volume ratio, which would be expected to trap peptides in close proximity to the comatrix (25).

We next epoxy-modified and conjugated nanodisks with antibodies specific to the 1,593.75 and 1,900.95 *m/z* peptides (*SI Appendix*, Fig. S8) to create a high-affinity, high-capacity peptide enrichment platform. Systematic analysis of MS signal enhancement by microwave digestion, nanodisk enrichment, and comatrix properties was performed with antigen-spiked healthy human serum, which was split and subjected to overnight or microwave-assisted trypsin digestion followed by MALDI-TOF MS analysis of nonimmunoprecipitated serum (no IP), peptides eluted from target-specific Dynabeads (Dynabead IP) or nanodisks (nanodisk IP), and peptides still bound to target-specific nanodisks (NanoDisk-MS) (Fig. 2*E*). *Mtb* target peptides were essentially undetectable in digests without IP, detected only weakly in microwave-assisted digests with conventional IP, but robustly detected when nanodisks were used for peptide enrichment or as an enrichment/comatrix platform.

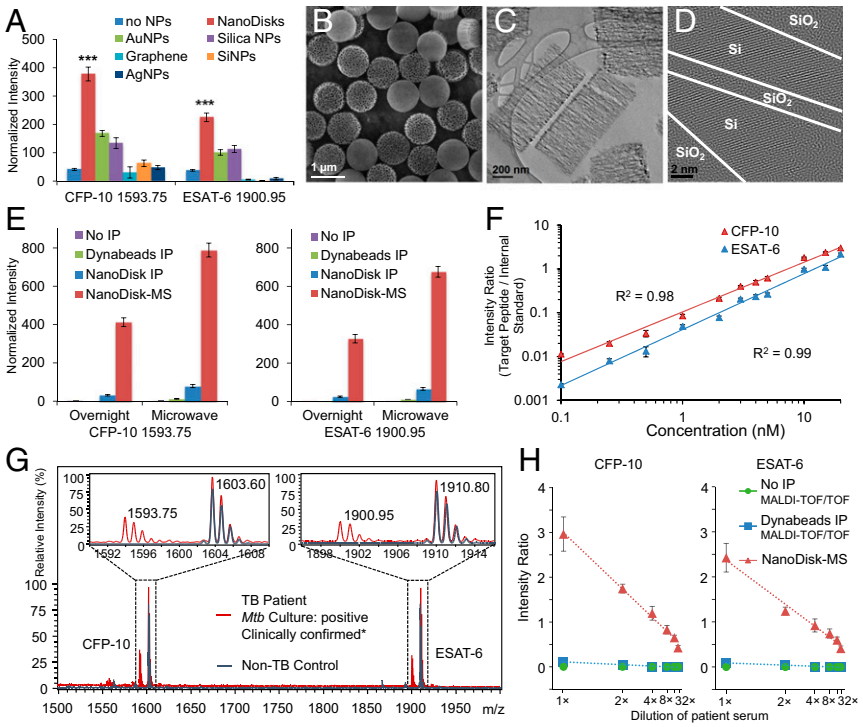

Fig. 2. Method optimization and multiplex quantification of *Mtb* target peptides. (*A*) MS signal intensity of target peptides analyzed alone (no NPs) or with graphene, silver (Ag), gold (Au), silicon (Si), silica nanoparticles (NPs), or nanodisks. (*B*) Scanning electron microscopy image of nanodisk structure. (*C* and *D*) Transmission electron microscopy images of cross-sectional structure (*C*) and silica modification (*D*) of nanodisk inner pore surfaces. (*E*) CFP-10 (*m/z* 1,593.75; *Left*) and ESAT-6 (*m/z* 1,900.95; *Right*) MS intensity in an antigen-spiked healthy serum sample that was trypsin-digested overnight (12 h) or by rapid microwave-irradiation (20 min) and then analyzed without IP, after IP and elution from target-specific Dynabeads or nanodisks, or by NanoDisk-MS. (*F*) Calibration curves for CFP-10 and ESAT-6 quantitation in serum ($n = 3$; $R^2 > 0.98$). (*G*) Representative MS spectra of CFP-10 and ESAT-6 peptides (*m/z* 1,593.75 and 1,900.95, respectively) and their internal standards (*m/z* 1,603.60 and 1,910.80, respectively) in serum of a healthy control (blue) and a TB case (red) analyzed by NanoDisk-MS. (*H*) CFP-10 (*Left*) and ESAT-6 (*Right*) MS intensity ratios of 1× (undiluted), 2×, 4×, 8×, 16×, and 32× diluted serum of a TB case analyzed by MALDI-TOF/TOF MS without IP, MALDI-TOF/TOF MS with Dynabead IP enrichment, and NanoDisk-MS. Data represent mean ± SEM. $n = 3$. ***$P < 0.001$.

The mean *Mtb* peptide signal was increased by 2.5-fold for CFP-10 and 2.6-fold for ESAT-6 by microwave-assisted digestion, by an additional 6.6-fold for both CFP-10 and ESAT-6 by nanodisk-mediated enrichment, and then by an additional 9.9-fold for CFP-10 and 10.2-fold for ESAT-6 by nanodisk comatrix activity.

Quantification of *Mtb*-Specific Peptides in Human Serum. TB-free human serum spiked with recombinant CFP-10 and ESAT-6 standards was digested under microwave irradiation, spiked with stable isotope-labeled internal standards, and analyzed by NanoDisk-MS. Calibration curves for antigen quantitation were generated by plotting the MS spectra intensity ratio between target peptides and internal standards against their respective input recombinant protein concentrations. Excellent correlation ($R^2 > 0.98$) was observed for curves made with different nanodisk batches (Fig. 2*F*), with values exhibiting 14–22% within-run and 16–23% between-run coefficients of variation. CFP-10 showed a 50 pM limit of detection (LOD) and a 200 pM limit of quantification (LOQ), ESAT-6 had a 200 pM LOD and a 500 pM LOQ, and measurement accuracies ranged from ∼74% (1 nM) to ∼90% (20 nM) (*SI Appendix*, Table S1). NanoDisk-MS also readily distinguished patients with TB and patients without TB in a proof-or-principle multiplex assay (Fig. 2*G*). Conversely, analyses performed using an advanced MALDI-TOF/TOF MS instrument failed to directly detect our target peptides in serially diluted serum of a TB patient with high CFP-10 (18 nM) and ESAT-6 (14 nM) levels, owing to the MALDI-inhibitory effects of serum sodium and lipids when no IP was performed and only weakly detected target signals after conventional IP with peptide-specific Dynabeads, which were lost after 2× serum dilution (Fig. 2*H*). In contrast, the NanoDisk-MS assays robustly detected both peptides in 2× serially diluted aliquots down to 32× dilution, demonstrating sufficient LOD in patients with low biomarker levels (Fig. 2*H*).

NanoDisk-MS Diagnostic Sensitivity and Specificity in an HIV-Negative Population. We assessed the diagnostic performance of NanoDisk-MS with serum of HIV-negative HTI patients, using a positive signal of either peptide as the TB diagnostic criterion. Cutoff values of CFP-10 concentration (200 pM) and ESAT-6 concentration (650 pM) were established before study initiation based on the maximum Youden index value in a development cohort including 25 active TB cases and 25 non-TB controls (*SI Appendix*, Fig. S9). Our case-control study contained 27 culture-positive PTB cases, 31 LTBI cases, 32 NTM cases, and 21 healthy controls. Blinded NanoDisk-MS assays detected target peptides in 25 of 27 (92.6%) TB cases (Table 1 and Fig. 3*A*), with 100% sensitivity in smear-positive cases and 91.0% sensitivity in smear-negative cases. No target signal was detected in the healthy controls, but false-positive signals were found in 4 of 31 LTBI cases (at risk) and in 3 of 32 NTM cases (disease control), for specificities of 87.1% and 90.6%, respectively. Notably, the LTBI signal may reveal subclinical TB cases, whereas NTM false-positive results may result from strains of three NTM species (*M. kansasii*, *M. marinum*, and *M. ulcerans*) that account for <5% of NTM cases (22), because the CFP-10 sequence of these two strains matches that of our target peptide (*SI Appendix*, Fig. S3*B*). LTBI follow-up and NTM strain analyses are needed to address these questions. However, *M. kansasii* cases were heavily overrepresented in our NTM group (13 of 32), and two of the three NTM false-positive cases had *M. kansasii* infection.

NanoDisk-MS Diagnostic Sensitivity and Specificity in an HIV-Positive Population. Noninvasive diagnosis of EPTB is challenging owing to the paucibacillary nature of patient sputum samples, and thus *Mtb* cultures are often done using more invasive specimens, including lymph nodes and pleural or cerebrospinal fluid. EPTB is particularly common in HIV/TB-coinfected patients, and HIV infection can disrupt pulmonary granulomas, which may reduce the utility of sputum-based diagnostic tests, whereas the altered immune responses in these patients may limit the utility of T-cell–mediated diagnostic assays (26).

We analyzed serum samples from HIV-positive HTI subjects with culture-positive or -negative PTB or EPTB. Blinded analyses identified 91.3% (21 of 23) and 82.4% (14 of 17) of the culture-positive and -negative PTB cases, respectively, and 92.3% (12 of 13) and 75.0% (6 of 8) of the culture-positive and -negative EPTB cases, respectively (Table 1 and Fig. 3*B*), while exhibiting 89.7% specificity (26 of 29) with TB-negative/HIV-positive subjects. NanoDisk-MS thus dramatically outperformed *Mtb* culture-based

Table 1. Sensitivity and specificity of NanoDisk-MS for active TB detection

HTI cohort (n = 201), group	Positive results/total no.	Sensitivity, % (95% CI)	Specificity, % (95% CI)
HIV$^-$ groups (n = 111)			
Pulmonary TB *Mtb* culture$^+$	25/27	92.6 (76.6–97.9)	
LTBI	4/31		87.1 (71.2–94.9)
NTM	3/32		90.6 (75.8–96.8)
Healthy controls	0/21		100 (84.5–100)
HIV$^+$ groups (n = 90)			
Pulmonary TB			
Mtb culture$^+$	21/23	91.3 (73.2–97.6)	
Mtb culture$^-$	14/17	82.4 (59.0–93.8)	
Extrapulmonary TB			
Mtb culture$^+$	12/13	92.3 (66.7–98.6)	
Mtb culture$^-$	6/8	75.0 (40.9–92.9)	
Non-TB	3/29		89.7 (73.6–96.4)

diagnosis of PTB (57.5%; 23 of 40) and EPTB (61.9%; 13 of 21) cases, and exhibited 100% and 84.3% sensitivity for smear-positive and -negative cases, respectively. These sensitivities also exceed those found in a study analyzing Xpert MTB/RIF sensitivities for culture-positive PTB cases (86.2%; 50 of 58) and culture-positive (67.7%; 21 of 31) and -negative (29.4%; 5 of 17) EPTB cases in a HIV-positive population (27).

Serum CFP-10 and ESAT-6 Levels in HIV-Infected Patients. HIV/TB-coinfected patients represent a demographically important TB population, because HIV-infected individuals are 20 times more likely to develop active TB disease (28, 29). Circulating *Mtb* antigen levels might be increased in these patients, however, as has been observed for other bacterial antigens (30). Indeed, combined CFP-10 + ESAT-6 levels were significantly higher in HIV-positive patients compared with HIV-negative patients with culture-positive PTB (9.8 nM vs. 3.3 nM) (Fig. 3*C*). NanoDisk-MS results are thus expected to permit robust TB diagnosis in HIV-positive patients with sensitivity exceeding that of most conventional methods (31).

Longitudinal Quantification of CFP-10 and ESAT-6 in Patients Receiving Anti-TB Therapy. Serum *Mtb* antigen concentrations during anti-TB therapy may reflect therapeutic efficacy. We analyzed serial blood samples from 9 HIV-negative and 12 HIV-positive TB patients during and after 6–12 mo of anti-TB therapy and follow-up. Serum *Mtb* peptide levels were decreased or undetectable in most HIV-negative (8 of 9) and HIV-positive (11 of 12) TB patients posttherapy (Fig. 4 and *SI Appendix*, Fig. S10*A*). The lone nonresponsive HIV-negative patient (ID no. 20020493) was found to have received an incomplete anti-TB regimen (11 of 20 monthly doses) owing to alcohol-induced liver dysfunction and to have exhibited consistent culture-positive results on a review of health records. One HIV-positive patient (ID no. 20020282) had a CFP-10 decrease that rebounded 2 mo after completion of therapy, perhaps owing to a lack of leukocyte bactericidal activity associated with G6PD deficiency or a decrease in the proportion of CD4$^+$ T lymphocytes (32). All of the other HIV-positive patients achieved *Mtb* antigen clearance during treatment or showed continued decreases posttreatment and ultimately had undetectable antigen levels.

We also collected samples from two prospectively enrolled patients with active TB before and shortly after the start of anti-TB therapy. Both patients exhibited significant *Mtb* antigen decreases by 9 d of treatment (*SI Appendix*, Fig. S10*B*), and were symptom- and culture-negative after 1 mo of treatment. Studies with larger longitudinal cohorts are underway to assess how early changes in antigen level correspond to symptom changes and treatment outcomes.

Discussion

Sustained and effective TB control is not exclusive to "third-world" countries—a lack of effective vaccines, emergence of drug-resistant TB strains, underperforming diagnostic strategies and slow culture-based therapy evaluation continue to cost millions of lives worldwide. The NanoDisk-MS assay described herein addresses sensitivity and speed issues associated with active TB diagnosis, and meets several criteria for a WHO-mandated noninvasive TB assay, because it (*i*) uses a small, noninvasive specimen; (*ii*) does not require bacterial isolation; (*iii*) has high sensitivity and specificity for active TB cases in extrapulmonary, culture-negative, and HIV-infected TB patients, for whom diagnosis often requires multiple tests, including invasive procedures; (*iv*) directly quantifies *Mtb* antigens for rapid monitoring of anti-TB therapy effects; (*v*) uses a streamlined process amenable to high-throughput operation in both clinical and research settings; and (*vi*) can be performed using equipment already approved by the Food and Drug Administration for other diagnostic assays.

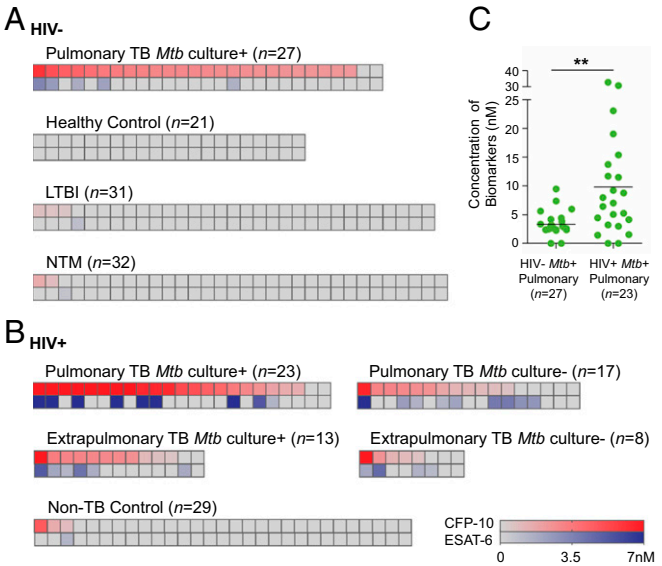

Fig. 3. Identification of active TB in adult patients. (*A* and *B*) Serum CFP-10 and ESAT-6 concentrations in adult HIV-negative (*A*) and HIV-positive (*B*) groups. Each column represents CFP-10 (upper cell, in red) and ESAT-6 (lower cell, in blue) results from a subject, ranked by high to low CFP-10 concentration. Antigen levels are indicated by the color intensity in the matching gradient bars. (*C*) Combined *Mtb* antigen (CFP-10 + ESAT-6) concentrations and means (black line) for the indicated groups. Data represent mean. n = 3. $^{**}P < 0.01$.

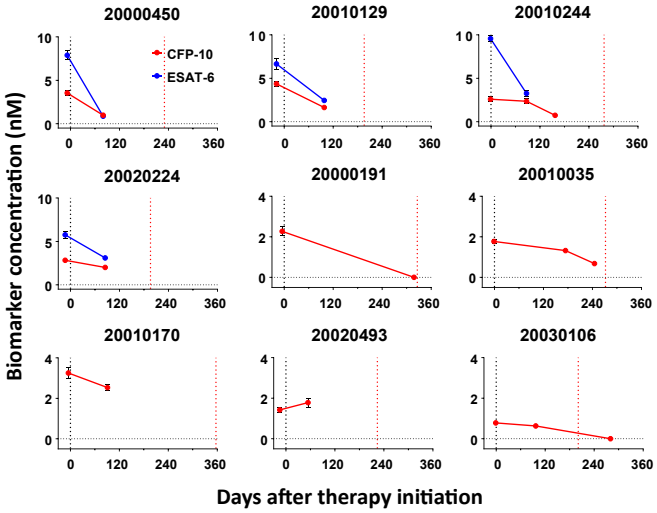

Fig. 4. Evaluation of anti-TB treatment efficacy. CFP-10 and ESAT-6 quantitation in archived serum samples of HIV-negative TB patients during anti-TB therapy (2–11 mo). Treatment start and end dates are indicated by blue and red dotted lines, respectively. Data represent mean ± SEM. $n = 3$.

We selected CFP-10 and ESAT-6 as biomarkers because they are known to modulate several key immunologic pathways to reduce mycobacterial clearance and promote host cell lysis, which may enhance *Mtb* dissemination. Thus, they may be more relevant than other abundant *Mtb* proteins, like antigen 85b, which is expressed by virulent and attenuated *Mtb* complex mycobacteria, including *M. bovis* bacillus Calmette–Guérin, to affect proliferation and perhaps uptake. Both CFP-10 and ESAT-6 are expressed by the RD-1 locus found in virulent but not attenuated *Mtb* complex strains, and RD-1 transfer into *M. bovis* bacillus Calmette–Guérin has been shown to increase virulence and survival (19). CFP-10 and ESAT-6 also appear to play important roles in the maintenance of *Mtb* infection by inhibiting mycobacterial clearance (33).

NanoDisk-MS demonstrated similar sensitivity for both PTB cases (87.5%) and clinically challenging EPTB cases (85.7%) in the HIV-positive study population, where it equaled or significantly outperformed Xpert MTB/RIF in terms of sensitivity for detecting EPTB using highly invasive lymph node (84%), pleural fluid (17%), and cerebrospinal fluid (56%) samples in a meta-analysis (34), and significantly outperformed AFB smear (31%), mycobacteria growth indicator tube culture (69%), and Xpert MTB/RIF (66%) in another study (35). Moreover, our results were achieved irrespective of *Mtb* culture status, and although greater sensitivity was achieved in culture-positive samples, results from culture-negative samples markedly outperformed the WHO-defined 66% optimal sensitivity for new high-priority nonsputum diagnostic tests (13). NanoDisk-MS also accurately diagnosed active TB cases in patients with HIV coinfection, which can adversely skew the results of blood-based host response immunoassays (e.g., IGRA and T-cell activation marker–tuberculosis assay) (26, 36), in which serum *Mtb* peptide concentrations were found to equal or exceed those found in HIV-negative subjects, supporting robust assay sensitivity. NanoDisk-MS exhibited differential specificities with healthy (100%) and HIV-positive (89.7%) controls, LTBI cases (87.1%), and NTM cases (90.6%), however. Owing to the increased TB risk in LTBI and HIV-positive groups and possible strain-specific NTM false-positives, longitudinal studies of LTBI and HIV-positive populations and strain identification of NTM cases are needed to further refine the specificity of the test in these groups.

NanoDisk-MS also was able to precisely quantify serum antigen concentrations, a highly desirable feature for monitoring responses to anti-TB therapy, given that assays currently used to monitor treatment response provide only qualitative or semi-quantitative results (smear and culture) or exhibit significant latency (Xpert). A study evaluating serial sputum samples from patients with smear-positive TB found that assay positivity and grade decreased linearly starting at ∼2 wk (smear), 4 wk (culture), or 6 wk (Xpert) posttreatment (37). $CD4^+$ T-cell responses also have been reported to differentiate LTBI and active TB cases and to monitor treatment responses, although only HIV-negative and culture- and/or smear-positive PTB patients were analyzed using this labor-intensive method, so that its clinical utility remains unclear (38). Circulating miRNA levels also may serve as TB biomarkers, but this idea has not yet been tested in longitudinal clinical studies (39). Results from proof-of-principle NanoDisk-MS studies analyzing *Mtb* peptide responses during anti-TB therapy detected marked reductions in both HIV-positive and -negative TB cases on initiation of anti-TB therapy, but these studies were not designed to measure rates of decline or for comparisons with other methods. Future prospective longitudinal studies with frequent sampling are needed to determine how *Mtb* peptide clearance corresponds to patient phenotypes and treatment outcomes. Should such a study confirm our preliminary results, the NanoDisk-MS assay would be expected improve the speed, accuracy, and efficiency of conventional procedures, which require months to estimate therapeutic efficacy or identify treatment resistance.

NanoDisk-MS was designed to enable multiplex detection of serum *Mtb* antigen concentrations for robust detection of active TB cases. Serum CFP-10 was detectable at lower concentrations than ESAT-6, perhaps owing to variable expression levels of ESAT-6 and CFP-10 in different strains of *Mtb* (40, 41). However, host β2 microglobulin also has been reported to bind ESAT-6 to mask a tryptic cleavage site (amino acids 90–95) required for the 1,900.95 *m/z* ESAT-6 peptide (16, 42), and thus may inhibit ESAT-6 cleavage to decrease the apparent serum ESAT-6 levels in our assay.

Nanodisk-MS requires only a simple, low-volume blood draw rather than invasive biopsies that may be required for other methods. Many hospitals and microbiology laboratories routinely use MALDI-TOF MS for microbial identification (43), which could allow rapid clinical translation of a NanoDisk-MS diagnostic assay. Further reductions in operator time and assay cost, along with improvements in instrument portability, are needed to meet WHO guidelines for an optimal noninvasive TB assay. Larger, randomized prospective studies are warranted to confirm the results of this proof-of-principle pilot study, but a clinical method that shares the advantages of our approach should facilitate earlier interventions and better patient outcomes (44). The NanoDisk-MS assay also opens up new possibilities for the diagnosis of a wide variety of other infectious diseases, because it should be relatively simple to generate similar assays to rapidly quantify disease-associated low-abundance antigens in blood and other body fluids.

Materials and Methods

Clinical Samples. The HTI cohort that served as a source of case and control samples in this study were the subjects of a large, population-based TB surveillance study that performed active surveillance of all confirmed TB cases in Houston/Harris County, Texas between 1995 and 2004. Because of its mandate to collect all active TB cases, the HTI archived samples from a variety of TB disease manifestations, including HIV-negative and -positive pulmonary and extrapulmonary TB cases with both positive and negative culture results. Serum samples were obtained from HTI subjects who were notified of the potential risks of study participation and provided written informed consent. Demographic, microbiology, and diagnostic data are summarized in *SI Appendix*, Table S2.

Microwave-Assisted and Overnight Tryptic Digestion of Human Serum Samples. Serum samples (100 μL) were mixed with 400 μL of 100 mM NH_4HCO_3 and 10 μL of 1 mg/mL sequencing-grade modified trypsin (Promega) in 1.5-mL Eppendorf tubes, placed in a 1,000-mL water bath, irradiated in a 1200 W microwave oven at 20% power for 20 min, and then mixed with a 0.1% final concentration of trifluoroacetic acid. Overnight trypsin digestions were incubated at 37 °C for 12 h using the same amount of trypsin and the same buffer conditions without a water bath and microwave irradiation.

Characterization, Functionalization, and Antibody Immobilization of Nanodisks. Bare nanodisks were fabricated following a previously reported protocol and stored in ACS grade 99.9% isopropyl alcohol for maximum stability (45). Functionalization details are reported in *SI Appendix, Materials and Methods*. Functionalized nanodisk suspensions (1 mL) were pelleted for 5 min at 10,000 × *g*, vacuum-dried, suspended in 1 mL of PBS (pH 8.6) containing 20 μg of anti-1593.75 or anti-1900.95 antibody (GL Biochem), mixed for 2 h at 25 °C, pelleted for 5 min at 10,000 × g, incubated for 30 min in 1 mL of 200 mM Tris pH 7/100 mM NaCl solution, washed three times with PBS (pH 7.4), pelleted and suspended in 60 μL of PBS (pH 7.4), and then stored at 4 °C until use (*SI Appendix*, Fig. S7*B*).

NanoDisk-MS Quantification of *Mtb* Antigens in Human Serum Samples. Standard curves were generated by spiking healthy donor serum with 0–100 nM recombinant CFP-10 or ESAT-6, subjected to microwave-assisted digestion and spiked with 10 nM stable isotope-labeled internal standard peptide (*m/z* 1,603.60 and 1,910.80; GenScript USA), mixed with antibody-conjugated nanodisks for 2 h, pelleted for 5 min at 10,000 × *g*, washed three times with 1 mg/mL 1,2-dioleoyl-sn-glycero-3-phospho-L-serine (Avanti Polar Lipids), suspended in 6 μL of deionized water and 4.5 μL (1.5 μL × 3) was analyzed by MALDI-TOF-MS, using the MS intensity ratios of each target peptide and internal standards. Clinical sample MS intensity ratios were converted to absolute molar concentrations through substitution into this calibration curve. The NanoDisk-MS assay is described in more detail in *SI Appendix, Materials and Methods*. Serum samples used to determine antigen-derived MS signals from trypsinized serum with or without Dynabead-mediated enrichment or NanoDisk-MS enrichment and comatrix activity were made by serially diluting TB patient serum with healthy human serum (2×, 4×, 8×, 16×, and 32×).

Statistical Analyses. GraphPad Prism 7 software was used to generate heat maps and to calculate one-way ANOVA with Bonferroni's posttest or Kruskal–Wallis one-way ANOVA with Dunn's posttest as determined by sample distribution and variance. Differences were considered statistically significant at $P < 0.05$. The diagnostic accuracy of tests were evaluated using the receiving operating characteristic curve. The cutoff values were estimated at various sensitivities and specificities and determined at the maximum Youden index value, that is, sensitivity + specificity − 1 (46). Data are presented as mean ± SEM unless noted otherwise.

ACKNOWLEDGMENTS. We thank Professor X. C. Li for helpful discussions and D. Hawk for excellent mass spectrometry technical assistance. This research was supported in part by National Institute of Allergy and Infectious Diseases Grants R01 AI113725-01A1 and R01 AI122932-01A1, the John S. Dunn Foundation, and the Intramural Research Programs of the NIH.

1. Zumla A, George A, Sharma V, Herbert N, Baroness Masham of Ilton (2013) WHO's 2013 global report on tuberculosis: Successes, threats, and opportunities. *Lancet* 382(9907): 1765–1767.
2. Marais BJ, Schaaf HS, Graham SM (2014) Child health and tuberculosis. *Lancet Respir Med* 2(4):254–256.
3. Monkongdee P, et al. (2009) Yield of acid-fast smear and mycobacterial culture for tuberculosis diagnosis in people with human immunodeficiency virus. *Am J Respir Crit Care Med* 180(9):903–908.
4. World Health Organization (2013) *Systematic Screening for Active Tuberculosis: Principles and Recommendations.* (WHO, Geneva).
5. Dunlap NE, et al. (2000) Diagnostic standards and classification of tuberculosis in adults and children. *Am J Respir Crit Care Med* 161(4 Pt 1):1376–1395.
6. Swaminathan S, Rekha B (2010) Pediatric tuberculosis: Global overview and challenges. *Clin Infect Dis* 50(Suppl 3):S184–S194.
7. Evans CA (2011) GeneXpert: A game-changer for tuberculosis control? *PLoS Med* 8(7): e1001064.
8. Ioannidis P, et al. (2011) Cepheid GeneXpert MTB/RIF assay for *Mycobacterium tuberculosis* detection and rifampin resistance identification in patients with substantial clinical indications of tuberculosis and smear-negative microscopy results. *J Clin Microbiol* 49(8):3068–3070.
9. World Health Organization (2014) *Xpert MTB/RIF: WHO Policy Update and Implementation Manual.* (WHO, Geneva).
10. Reid MJA, Shah NS (2009) Approaches to tuberculosis screening and diagnosis in people with HIV in resource-limited settings. *Lancet Infect Dis* 9(3):173–184.
11. Horne DJ, et al. (2010) Sputum monitoring during tuberculosis treatment for predicting outcome: Systematic review and meta-analysis. *Lancet Infect Dis* 10(6):387–394.
12. Denkinger CM, Pai M, Patel M, Menzies D (2013) Gamma interferon release assay for monitoring of treatment response for active tuberculosis: An explosion in the spaghetti factory. *J Clin Microbiol* 51(2):607–610.
13. World Health Organization (2014) *High-Priority Target Product Profiles for New Tuberculosis Diagnostics: Report of a Consensus Meeting.* (WHO, Geneva).
14. Centers for Disease Control and Prevention (2010) Updated guidelines for using interferon gamma release assays to detect *Mycobacterium tuberculosis* infection—United States. *MMWR Recomm Rep* 59(RR-5):1–25.
15. Sweeney TE, Braviak L, Tato CM, Khatri P (2016) Genome-wide expression for diagnosis of pulmonary tuberculosis: A multicohort analysis. *Lancet Respir Med* 4(3): 213–224.
16. Sreejit G, et al. (2014) The ESAT-6 protein of *Mycobacterium tuberculosis* interacts with beta-2-microglobulin (β2M) affecting antigen presentation function of macrophage. *PLoS Pathog* 10(10):e1004446.
17. Simossis VA, Heringa J (2003) The PRALINE online server: Optimising progressive multiple alignment on the web. *Comput Biol Chem* 27(4-5):511–519.
18. van Ingen J, de Zwaan R, Dekhuijzen R, Boeree M, van Soolingen D (2009) Region of difference 1 in nontuberculous *Mycobacterium* species adds a phylogenetic and taxonomical character. *J Bacteriol* 191(18):5865–5867.
19. Cardona P-J (2012) *Understanding Tuberculosis: Deciphering the Secret Life of the Bacilli* (In Tech, Rijeka, Croatia).
20. Feng TT, et al. (2011) Novel monoclonal antibodies to ESAT-6 and CFP-10 antigens for ELISA-based diagnosis of pleural tuberculosis. *Int J Tuberc Lung Dis* 15(6):804–810.
21. Arend SM, et al. (2002) Tuberculin skin testing and in vitro T cell responses to ESAT-6 and culture filtrate protein 10 after infection with *Mycobacterium marinum* or *M. kansasii*. *J Infect Dis* 186(12):1797–1807.
22. Lai CC, et al. (2010) Increasing incidence of nontuberculous mycobacteria, Taiwan, 2000-2008. *Emerg Infect Dis* 16(2):294–296.
23. Tirumalai RS, et al. (2003) Characterization of the low molecular weight human serum proteome. *Mol Cell Proteomics* 2(10):1096–1103.
24. Sun W, et al. (2006) Microwave-assisted protein preparation and enzymatic digestion in proteomics. *Mol Cell Proteomics* 5(4):769–776.
25. Wei J, Buriak JM, Siuzdak G (1999) Desorption-ionization mass spectrometry on porous silicon. *Nature* 399(6733):243–246.
26. Portevin D, et al. (2014) Assessment of the novel T-cell activation marker-tuberculosis assay for diagnosis of active tuberculosis in children: A prospective proof-of-concept study. *Lancet Infect Dis* 14(10):931–938.
27. Zeka AN, Tasbakan S, Cavusoglu C (2011) Evaluation of the GeneXpert MTB/RIF assay for rapid diagnosis of tuberculosis and detection of rifampin resistance in pulmonary and extrapulmonary specimens. *J Clin Microbiol* 49(12):4138–4141.
28. Getahun H, Gunneberg C, Granich R, Nunn P (2010) HIV infection-associated tuberculosis: The epidemiology and the response. *Clin Infect Dis* 50(Suppl 3):S201–S207.
29. Abeyewickreme I, Punchihewa N, Maw-Naing A (2012) Success of tuberculosis and HIV collaboration. *WHO South-East Asia J Public Health* 1(4):359–361.
30. Jiang W, et al. (2009) Plasma levels of bacterial DNA correlate with immune activation and the magnitude of immune restoration in persons with antiretroviral-treated HIV infection. *J Infect Dis* 199(8):1177–1185.
31. Theron G, et al. (2011) Evaluation of the Xpert MTB/RIF assay for the diagnosis of pulmonary tuberculosis in a high HIV prevalence setting. *Am J Respir Crit Care Med* 184(1):132–140.
32. Schilirò G, Minniti C, Sciotto A, Bellino A, Russo A (1986) T-lymphocyte subpopulation changes during hemolysis in glucose-6-phosphate dehydrogenase (G6PD)-deficient children. *Am J Hematol* 21(2):173–176.
33. Prendergast KA, et al. (2016) The Ag85B protein of the BCG vaccine facilitates macrophage uptake but is dispensable for protection against aerosol *Mycobacterium tuberculosis* infection. *Vaccine* 34(23):2608–2615.
34. World Health Organization (2013) *Policy Update: Xpert MTB/RIF Assay for the Diagnosis of Pulmonary and Extrapulmonary TB in Adults and Children.* (WHO, Geneva).
35. Cavanaugh JS, et al. (2016) Comparative yield of different diagnostic tests for tuberculosis among people living with HIV in western Kenya. *PLoS One* 11(3):e0152364.
36. Mandalakas AM, et al. (2008) High level of discordant IGRA results in HIV-infected adults and children. *Int J Tuberc Lung Dis* 12(4):417–423.
37. Friedrich SO, et al.; Pan African Consortium for the Evaluation of Anti-tuberculosis Antibiotics (PanACEA) (2013) Assessment of the sensitivity and specificity of Xpert MTB/RIF assay as an early sputum biomarker of response to tuberculosis treatment. *Lancet Respir Med* 1(6):462–470.
38. Adekambi T, et al. (2015) Biomarkers on patient T cells diagnose active tuberculosis and monitor treatment response. *J Clin Invest* 125(5):1827–1838.
39. Zhang H, et al. (2014) Identification of serum microRNA biomarkers for tuberculosis using RNA-seq. *PLoS One* 9(2):e88909.
40. Uplekar S, Heym B, Friocourt V, Rougemont J, Cole ST (2011) Comparative genomics of Esx genes from clinical isolates of *Mycobacterium tuberculosis* provides evidence for gene conversion and epitope variation. *Infect Immun* 79(10):4042–4049.
41. Arend SM, et al. (2005) ESAT-6 and CFP-10 in clinical versus environmental isolates of *Mycobacterium kansasii*. *J Infect Dis* 191(8):1301–1310.
42. Teutschbein J, et al. (2009) A protein linkage map of the ESAT-6 secretion system 1 (ESX-1) of *Mycobacterium tuberculosis*. *Microbiol Res* 164(3):253–259.
43. Patel R (2013) MALDI-TOF mass spectrometry: Transformative proteomics for clinical microbiology. *Clin Chem* 59(2):340–342.
44. Denkinger CM, Grenier J, Minion J, Pai M (2012) Promise versus reality: Optimism bias in package inserts for tuberculosis diagnostics. *J Clin Microbiol* 50(7):2455–2461.
45. Godin B, et al. (2012) Discoidal porous silicon particles: Fabrication and biodistribution in breast cancer bearing mice. *Adv Funct Mater* 22(20):4225–4235.
46. Youden WJ (1950) Index for rating diagnostic tests. *Cancer* 3(1):32–35.